PROCEEDINGS OF SPIE
SPIE—The International Society for Optical Engineering

Smart Structures and Materials 2000

Mathematics and Control in Smart Structures

Vasundara V. Varadan
Chair/Editor

6–9 March 2000
Newport Beach, USA

Sponsored by
SPIE—The International Society for Optical Engineering

Cosponsored by
SEM—Society for Experimental Mechanics
American Society for Mechanical Engineers
BFGoodrich (USA)
DARPA—Defense Advanced Research Projects Agency (USA)
U.S. Army Research Office

Cooperating Organizations
Air Force Research Laboratory (USA)
The Ceramic Society of Japan
Intelligent Materials Forum (Japan)

Published by
SPIE—The International Society for Optical Engineering

Volume 3984

Control of a directly-excited structural dynamic model of an F-15 tail section using positive position feedback

Ayman A. El-Badawy* and Ali H. Nayfeh†

Virginia Polytechnic Institute and State University
Blacksburg, VA 24061–0219

ABSTRACT

We investigated the use of positive position feedback (PPF) to suppress high-amplitude vibrations of a structural dynamic model of a twin-tail assembly of the F-15 fighter when subjected to primary resonance excitations. We developed the nonlinear differential equations of motion and obtained an approximate solution using the method of multiple scales. Then, we conducted bifurcation analyses for the open- and closed-loop response of the system and investigated theoretically the performance of the control strategy. The theoretical findings indicate that the control law leads to an effective vibration suppression and bifurcation control. We conducted experiments to verify the theoretical analysis. We built a digital control system that consists of the SIMULINK modeling software and a dSPACE controller installed in a personal computer, and we used actuators made of piezoelectric ceramic material. The experimental results show that PPF is effective in suppressing the steady-state vibrations.

Key Words: F-15, twin-tails, vibration absorber, perturbation, control.

1 INTRODUCTION

Buffeting is defined as the response of aircraft structures (such as wings and tails) to unsteady flow[1]. A typical fighter aircraft, such as the F-15, performs maneuvers at high angles of attack. Depending on the angle of attack and the freestream velocity, vortical flows impinge on the tails and create large dynamic responses, which result in large dynamic loads and stresses throughout the tail structure. These loads may excite different vibration modes that cause severe structural fatigue damage and premature failure. Thus it is important to reduce the unwanted vibrations caused by buffet loads and thus extend the fatigue life of the F-15 vertical tails.

*Graduate student.
†University Distinguished Professor.

In *Smart Structures and Materials 2000: Mathematics and Control in Smart Structures*, Vasundara V. Varadan, Editor, Proceedings of SPIE Vol. 3984 (2000) • 0277-786X/00/$15.00

From a structural viewpoint, the tail can be approximated by a cantilevered beam, and one can find examples of various active control schemes for this type of element in the literature. Our goal is to enhance the damping of targeted vibration modes. As an alternative to state variable feedback, many authors have suggested the use of second-order compensation in the feedback loop. There exist robust and efficient methods for this type of control, such as the positive position feedback of Goh and Caughey[2] and the active vibration absorber of Juang and Phan[3]. Second-order compensators have been proposed to provide loop-shaping control of structures using collocated sensor-actuator pairs. In these approaches, the compensator is used to increase the damping of a targeted structural mode in a fashion analogous to a mechanical vibration absorber.

Most of the papers in the literature deal with either only one tail counting on symmetry or two tails one rigid and the other flexible. These papers thus miss the interaction between the two tails. According to Ferman et al.[4], the structural response characteristics of the left and right vertical tails of the F-15 aircraft are distinctly different. This is primarily due to the difference in the size of the tip pods, with the left tail being more prone to fatigue than the right tail.

In this work, we investigate the influence of two PPF filters on the response of the two tails of the scaled structural dynamic model . The advantages of PPF control lie in the fact that the actuator dynamics are ignorable, it is based on physical quantities that can be measured accurately (i.e., the system natural frequencies), and it is amenable to strain-based actuation which makes it an excellent choice for smart structure applications. For this investigation, we use piezoceramics actuators to control the forced vibrations of the first modes of the twin tails. We describe and demonstrate the roles of the filter parameters and the feedback gain on the response of the twin tails.

2 THEORETICAL DEVELOPMENT

The closed-loop response of the twin tails to a primary resonance excitation can be modeled by two mass-normalized second-order coupled differential equations, while the dynamics of the two filters can be modeled by two second-order differential equations. The first filter targets the response of the right tail, while the second filter targets the response of the left tail. The governing equations can be written as

$$\ddot{u}_1 + \omega_1^2 u_1 + 2\epsilon\mu_1\dot{u}_1 + \epsilon\alpha_1 u_1^3 + \epsilon\mu_3\dot{u}_1 \mid \dot{u}_1 \mid -\epsilon k(u_2 - u_1) = \epsilon F\cos(\Omega t + \tau_1) + \epsilon\rho_1 u_3 \tag{1}$$

$$\ddot{u}_2 + \omega_2^2 u_2 + 2\epsilon\mu_2\dot{u}_2 + \epsilon\alpha_2 u_2^3 + \epsilon\mu_4\dot{u}_2 \mid \dot{u}_2 \mid -\epsilon k(u_1 - u_2) = \epsilon F\cos(\Omega t + \tau_2) + \epsilon\rho_2 u_4 \tag{2}$$

$$\ddot{u}_3 + 2\epsilon\zeta_3\dot{u}_3 + \omega_3^2 u_3 = \epsilon\rho_3 u_1 \tag{3}$$

$$\ddot{u}_4 + 2\epsilon\zeta_4\dot{u}_4 + \omega_4^2 u_4 = \epsilon\rho_4 u_2 \tag{4}$$

where u_1 and u_2 denote the generalized coordinates of the first bending modes of the twin-tail assembly, u_3 and u_4 denote the filters coordinates, ω_1 and ω_2 are the lowest linear natural frequencies of the right and left tails,

ω_3 and ω_4 are the frequencies of the filters, μ_1, μ_2, ζ_3, and ζ_4 are the linear damping coeffecients, α_1 and α_2 are the coeffecients of the cubic nonlinearity, μ_3 and μ_4 are aerodynamic damping coefficients, k is the coupling coefficient of the twin tails, and $F\cos(\Omega t+\tau_1)$ and $F\cos(\Omega t+\tau_2)$ are the direct excitations of the tail section. Here, ϵ is a bookkeeping parameter, which can be set equal to unity in the final analysis. The parameters in equations (1)-(4) were identified using experimental data[5]. They are listed in Appendix I. A collocated strain measurment is available, and thus we use $\rho_1 = G_1\omega_1^2$, $\rho_2 = G_2\omega_2^2$, $\rho_3 = \omega_3^2$, and $\rho_4 = \omega_4^2$, where G_1 and G_2 are feedback gains.

Using the method of multiple scales[6], we determined the equations governing the modulation of the amplitudes and phases of the modes. The result is

$$p_1' = -\mu_1 p_1 + \frac{1}{2\omega_1}\eta_1 k q_1 - \nu_1 q_1 + \frac{3}{8\omega_1}\alpha_1 p_1^2 q_1 + \frac{3}{8\omega_1}\alpha_1 q_1^3 - \frac{1}{2\omega_1}\eta_1 k q_2 - \frac{4}{3\pi}\mu_3\omega_1\sqrt{p_1^2+q_1^2}\,p_1 - \frac{\rho_1}{2\omega_1}q_3 \tag{5}$$

$$q_1' = \frac{F}{2\omega_1} - \frac{1}{2\omega_1}\eta_1 k p_1 + \nu_1 p_1 - \frac{3}{8\omega_1}\alpha_1 p_1^3 + \frac{1}{2\omega_1}\eta_1 k p_2 - \mu_1 q_1 - \frac{3}{8\omega_1}\alpha_1 p_1 q_1^2 - \frac{4}{3\pi}\mu_3\omega_1\sqrt{p_1^2+q_1^2}\,q_1 + \frac{\rho_1}{2\omega_1}p_3 \tag{6}$$

$$p_2' = -\mu_2 p_2 + \frac{1}{2\omega_1}\eta_2 k q_1 - 4k\eta_2 q_2 - \nu_2 q_2 + \frac{3}{8\omega_2}\alpha_2 p_2^2 q_2 + \frac{3}{8\omega_2}\alpha_2 q_2^3 - \frac{4}{3\pi}\mu_3\omega_1\sqrt{p_1^2+q_1^2}\,p_1 - \frac{\rho_2}{2\omega_2}q_4 \tag{7}$$

$$q_2' = \frac{F}{2\omega_2} + \frac{1}{2\omega_2}\eta_2 k p_1 - \frac{1}{2\omega_2}\eta_2 k p_2 + \nu_2 p_2 - \frac{3}{8\omega_2}\alpha_2 p_2^3 - \mu_2 q_2 - \frac{3}{8\omega_2}\alpha_2 p_2 q_2^2 - \frac{4}{3\pi}\mu_4\omega_2\sqrt{p_2^2+q_2^2}\,q_2 + \frac{\rho_2}{2\omega_2}p_4 \tag{8}$$

$$p_3' = -\zeta_3 p_3 - \frac{\rho_3}{2\omega_3}q_1 - \nu_3 q_3 \tag{9}$$

$$q_3' = \frac{\rho_3}{2\omega_3}p_1 + \nu_3 p_3 - \zeta_3 q_3 \tag{10}$$

$$p_4' = -\zeta_4 p_4 - \frac{\rho_4}{2\omega_4}q_2 - \nu_4 q_4 \tag{11}$$

$$q_4' = \frac{\rho_4}{2\omega_4}p_2 + \nu_4 p_4 - \zeta_4 q_4 \tag{12}$$

The performance of the control was evaluated by calculating the equilibrium solutions of equations (5)-(12) and examining their stability as a function of the frequency of excitation and the gains G_i. Thus, we set the time derivatives in equations (5)-(12) equal to zero and solved the resulting system of algebraic equations for the p_i and q_i for a specified value of one of the parameters. The amplitudes a_1, a_2, a_3, and a_4 of the responses of the two tails and the two filters were then calculated from $a_i = \sqrt{p_i^2+q_i^2}$. Since there is no closed-form solution for the eight algebraic equations, we resorted to numerical techniques. Numerical integration of the modulation equations for different sets of initial conditions was used to locate some of the possible solutions for a given frequency and amplitude of excitation. Then, starting with these solutions, we used a pseudo-arclength scheme[7] to trace the branches of the equilibrium solutions by varying the excitation frequency.

The stability of a particular equilibrium solution was determined by examining the eigenvalues of the Jacobian matrix of the right-hand sides of equations (5)-(12). If the real part of each eigenvalue is negative, the corresponding equilibrium solution is asymptotically stable. If the real part of any of the eigenvalues is positive, the corresponding equilibrium solution is unstable. In the next two sections, we perform the stability analysis and evaluate the control law.

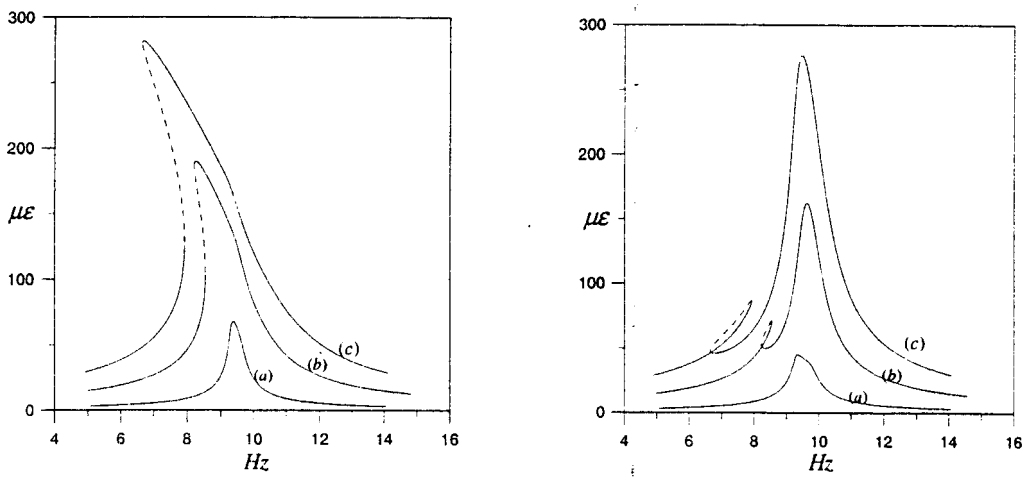

(i) right-tail response

(ii) left-tail response

Figure 1: Effect of varying the excitation amplitude on the frequency-response curves of the two tails: a) F=0.33g, b) F=1.65g, and c) F=3.3g.

3 THEORETICAL FREQUENCY-RESPONSE CURVES

In Fig. 1, we show frequency-response curves for the open-loop case for various levels of the excitation amplitude. The amplitude of the response depends on the detuning and amplitude of the excitation. Solid lines correspond to stable solutions, while dashed lines correspond to unstable solutions. All of the bifurcations are saddle-node bifurcations. For the right tail, it is clear that, as the amplitude of excitation increases, the frequency-response curves bend away from the linear curves, resulting in multivalued regions. The multivaluedness is responsible for jumps. The left tail has multivalued responses in the region between 6-8 Hz. We note here that, as the forcing amplitude increases, the nonlinearity will dominate the response. In fact, twin-tail aircraft are often subjected to high-intensity buffet loads that produce accelerations in excess of 450g at the tip of the vertical tail during maneuvers at high angles of attacks[8].

3.1 Effect of varying the damping and the feedback gain

Figures 2 and 3 show the frequency-response curves of the two tails and the two absorbers. Here, the frequency of each absorber is set equal to the natural frequency of the first mode of the corresponding tail. In these figures, curves for different values of the damping ratios of the two absorbers are plotted. It is clear that, as the damping is increased, the resonant response is reduced at the expense of increasing the response amplitude. If the damping is decreased, the response amplitudes of the tails and the absorbers increase, which might set a limitation on the

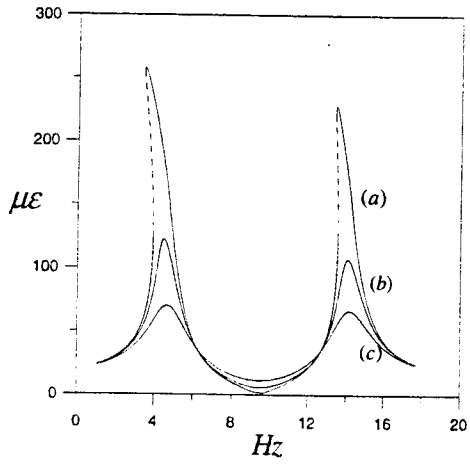

(i) right-tail response

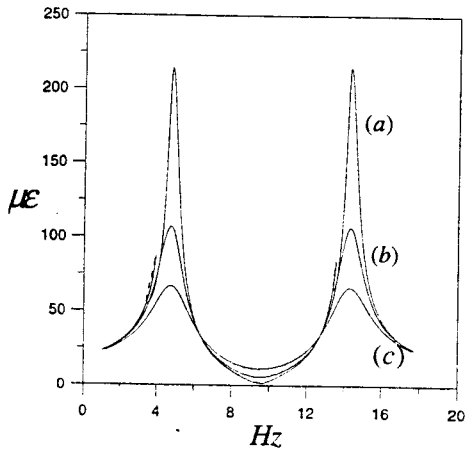

(ii) left-tail response

Figure 2: Effect of varying the damping ratios of the two absorbers on the frequency-response curves of the two tails while fixing the values of the frequencies of the two absorbers ($\sigma_3 = \sigma_4 = 0$, $F = 3.3g$): a) $\zeta_{3,4} = 0.01$, b) $\zeta_{3,4} = 0.1$, and c) $\zeta_{3,4} = 0.2$.

operation of the actuator, especially during a frequency sweep. Thus there is this tradeoff between the amplitude response of the tails and the possibility of saturating the absorbers.

To eliminate the introduction of unwanted absorber damping, Hollkamp and Starchville[9] used a linear self-tuning PZT absorber. They used a computer that senses the frequency of the structure and through a motor driven potentionmeter, adjusts the shunt's frequency to optimize the absorber performance. Oueini et al.[10], on the other hand, developed a code that automated the implementation of the absorber by the use of a digital signal processing (DSP) board that tracks the plant's frequency of oscillation. If this is the case, then resorting to an absorber with low damping is preferable since the amplitude response of the tails will be minimum.

Figures 4 and 5 show frequency-response curves of the two tails and the two absorbers the frequencies of the absorbers being automatically tuned to the excitation frequency. To theoretically implement this, for example for the right tail, we set $\Omega = \omega_1 + \sigma_1$ and $\omega_3 = \omega_1 + \sigma_3$, where Ω is the excitation frequency, ω_1 is the natural frequency of the right tail, and ω_3 is the frequency of the absorber. The latter is tuned to the response frequency of the first modeof the right tail. If we set $\sigma_3 = \sigma_1$ (i.e., the absorber frequency is equal to the excitation frequency) during a frequency sweep, we obtain Fig. 4 (i). A similar analysis was done for the left tail. We note that σ_2 is fixed and is equal to $\omega_2 - \omega_1 = 0.085$Hz.

Figures 6 and 7 show the effect of varying the feedback gain on the responses of the tails and the absorbers. These figures were obtained while tuning the frequencies of the absorbers to be equal to the excitation frequency (i.e., $\Omega = \omega_3$) and a damping ratio $\zeta_{3,4} = 0.2$. As the the gain increases, the responses of the tails and the absorbers

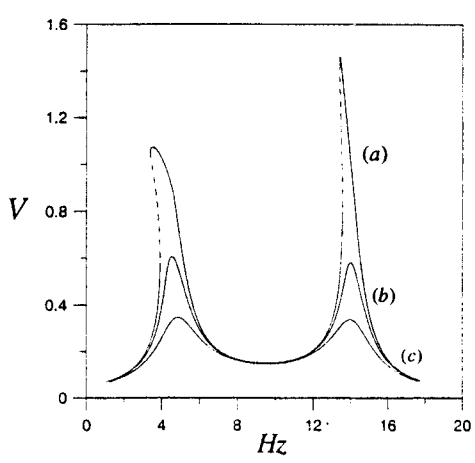

(i) right-tail absorber response

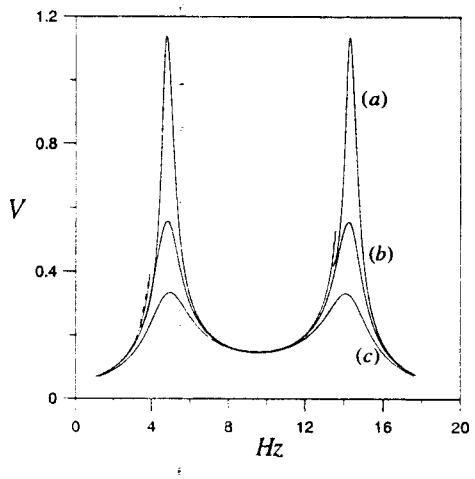

(ii) left-tail absorber response

Figure 3: Effect of varying the damping ratios of the two absorbers on their frequency-response curves while fixing their frequencies($\sigma_3 = \sigma_4 = 0$, $F = 3.3g$): a) $\zeta_{3,4} = 0.01$, b) $\zeta_{3,4} = 0.1$, and c) $\zeta_{3,4} = 0.2$.

decrease. However, from the experiments, we found that, although this is true, the system loses stability when the gain increases beyond a threshold value. Thus, one should be careful in selecting the feedback gains so as not destabilize the system.

4 EXPERIMENTS

To test the control method, we built a digital control system using the SIMULINK modeling software[11] and a dSPACE controller[12] in a personal computer. The SIMULINK software is used to build the control block diagram, and then the dSPACE real-time workshop is used to generate a C-code from the SIMULINK model. The C-code is then connected by the dSPACE real-time interface to the dSPACE real-time hardware system.

4.1 Setup

The tail section used in the experiments is a 1/16 dynamically scaled model of the F-15 tail assembly. The model was constructed at the laboratory of Professor Sathya Hanagud at the Georgia Institute of Technology from a series of aluminum channels, brass rings, composite plates, metal masses, and various adhesives, as shown in Fig. 8 (i). The model is approximately 0.355 m long, 0.228 m tall, and 0.482 m wide.

Figure 8 (ii) shows the experimental setup. The tail deflections were measured with a series of four strain

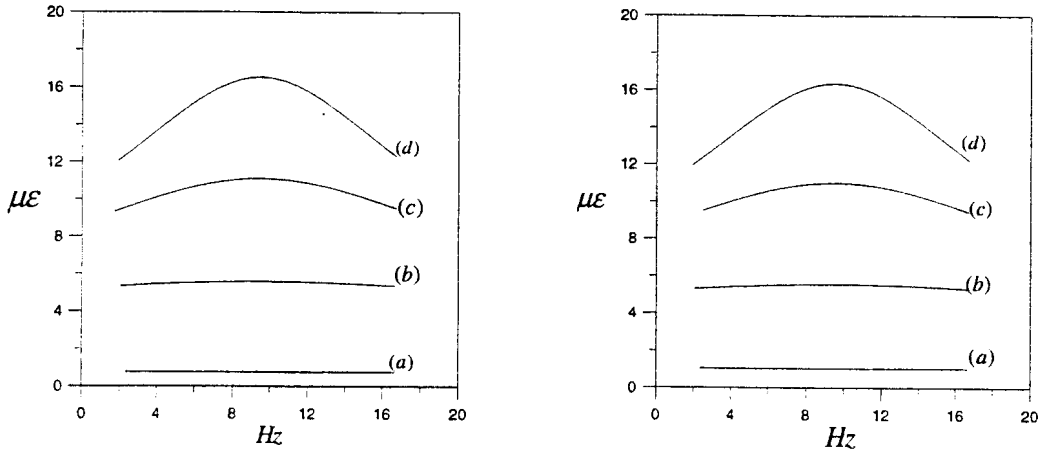

(i) right-tail response

(ii) left-tail response

Figure 4: Effect of varying the damping ratios of the two absorbers on the frequency-response curves of the two tails (F=3.3g): a) $\zeta_{3,4}$=0.01, b) $\zeta_{3,4}$=0.1, c) $\zeta_{3,4}$=0.2, and d) $\zeta_{3,4}$=0.3.

gages. The centers of the gage pairs were 0.9 *cm* and 8.5 *cm* from the top of the aluminum channels. One pair was placed on the outside of the right vertical tail; the other pair was placed on the outside of the left vertical tail. The strain gages were aligned to measure the bending moments. Changes in the gages were measured with a strain-gage conditioning amplifier in a quarter bridge configuration. The actuators were two piezoelectric patches made from lead-zirconate-titanate. One patch was placed near the root of each tail. The dimensions of the patches are $7 \times 3.5 \times .019$ *cm*.

A series of bolts and several positioning blocks were used to fix the model. The tails were actuated by placing two PZT patches on the inner sides of the tails. The tails were excited by two other PZT patches placed on the outer sides of the tails.

The responses of the tails and the controller signals were monitored using a four-channel signal analyzer and an oscilloscope. The responses were also collected by a data acquisition computer software. The strain-gage signal from the conditioner was fed to the controllers, and the control signal was generated, amplified, and sent to the actuators. The technique was implemented using a Runge-Kutta integrator with a data sampling period of $T = 0.0005$.

4.2 Experimental results

The maximum tail vibration achieved with the PZT actuators was $0.33V \approx 62\mu\epsilon$, which is in the linear response range of the tails (refer to Fig. 1). However, the results can be generalized to the full nonlinear system

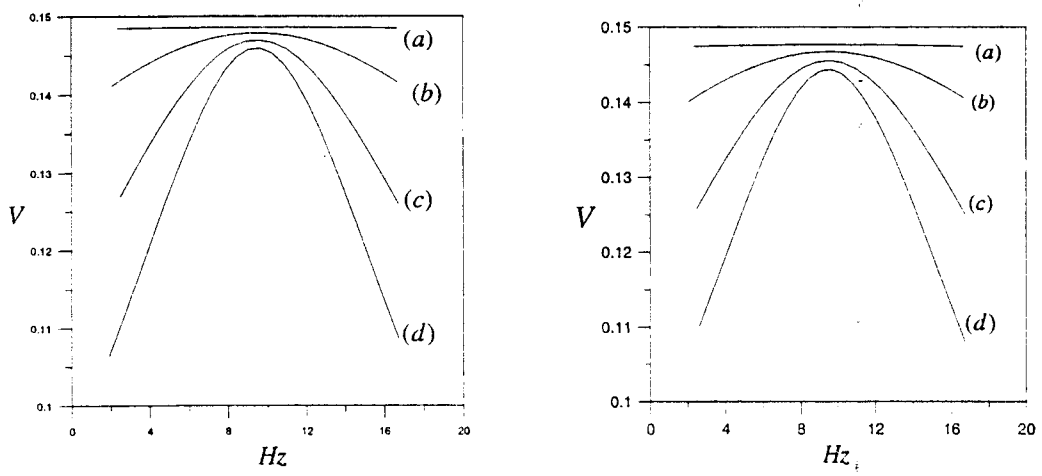

(i) right-tail absorber response

(ii) left-tail absorber response

Figure 5: Effect of varying the damping ratios of the two absorbers on their frequency-response curves (F=3.3 g): a) $\zeta_{3,4}$=0.01, b) $\zeta_{3,4}$=0.1, c) $\zeta_{3,4}$=0.2, and d) $\zeta_{3,4}$=0.3.

because the mathematical model describing the dynamics of the tails is fairly accurate[5]. Figures 9 and 10 show the time histories and the FFT of the open- and closed-loop responses of the right tail. Similar results were obtained for the left tail. It is clear that the amplitudes of the responses are reduced by almost 10 times.

Using a larger feedback gain, one can reduce the transient time required to reach steady state and at the same time reduce the steady-state amplitude. However, since the control force is generated by the tail vibration itself, the controller vibration amplitude can never approach zero. In fact, the system becomes unstable when the gain increases beyond a certain value. Figure 11 shows the control signal sent to the power amplifier, which in turn was sent to the PZT actuators. In this figure, the system is actually on the verge of instability. Increasing the feedback gain slightly would increase the modulation of the control signal, which would lead to an unstable system.

5 CONCLUSIONS

A positive postion-feedback control was used to suppress the vibrations of the first bending modes of the twin tails of a 1/16 structural dynamic model of an F-15 twin-tail assembly when subjected to primary resonance excitations. The dynamics of the first flexural modes of the twin tails were modeled by two second-order coupled nonlinear ordinary-diffferential equations. A filter was coupled linearly to each of the tails. The method of multiple scales was used to derive eight first-order differential equations governing the amplitudes and phases of the response. Then a bifurcation analysis was conducted to examine the stability of the closed-loop system and

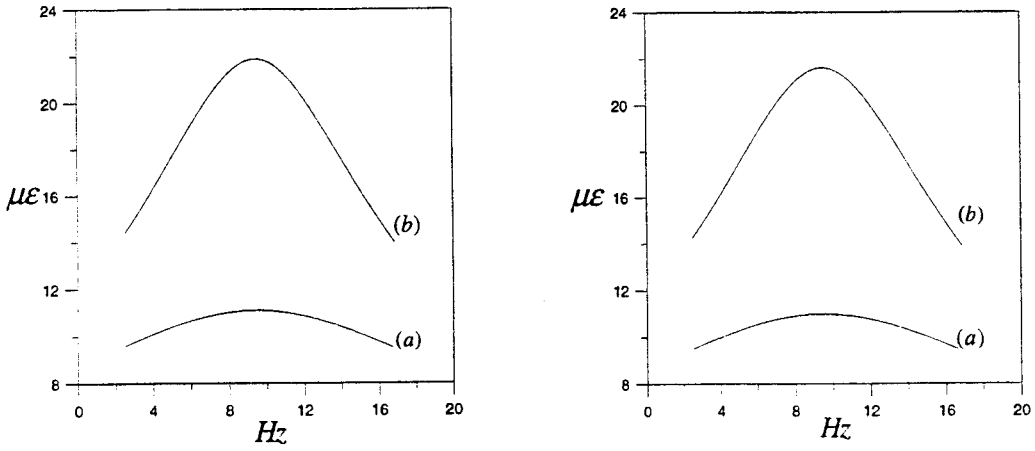

(i) right-tail response

(ii) left-tail reponse

Figure 6: Effect of varying the feedback gain on the frequency-response curves of the two tails while fixing the values of the frequencies of the two absorbers ($\zeta_{3,4}$=0.2, F=3.3g): a) G=1 and b) G=0.5.

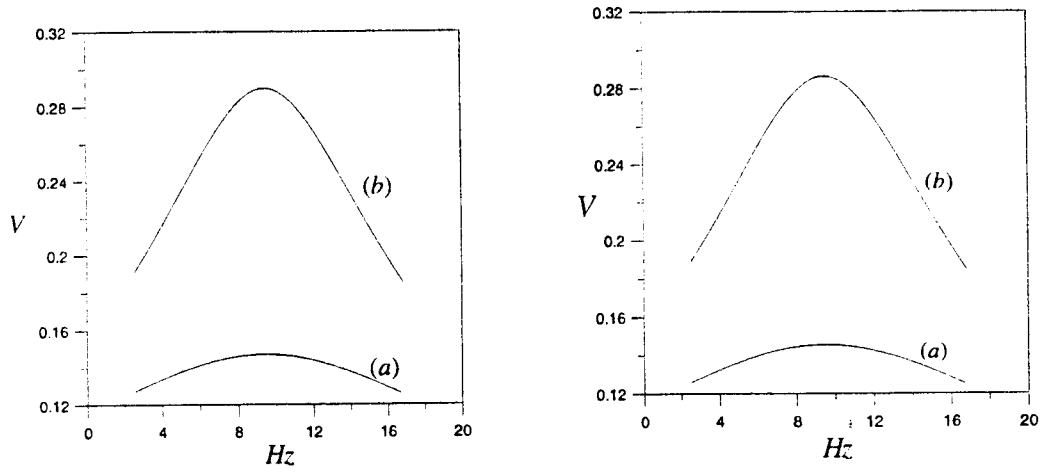

(i) right-tail absorber response

(ii) left-tail absorber response

Figure 7: Effect of varying the feedback gain on the frequency-response curves of the two absorbers while fixing the values of their frequencies ($\zeta_{3,4}$=0.2, F=3.3g): a) G=1 and b) G=0.5.

investigate the performance of the control law. The control eliminated all multiple responses. The amplitudes of oscillation of the tails decreased significantly. Once the absorbers frequencies are properly tuned, we show that the control scheme possesses a wide suppression bandwidth. Also, a parametric investigation was carried out to investigate the effect of changing the damping ratios of the absorbers and the value of the feedback gain on the

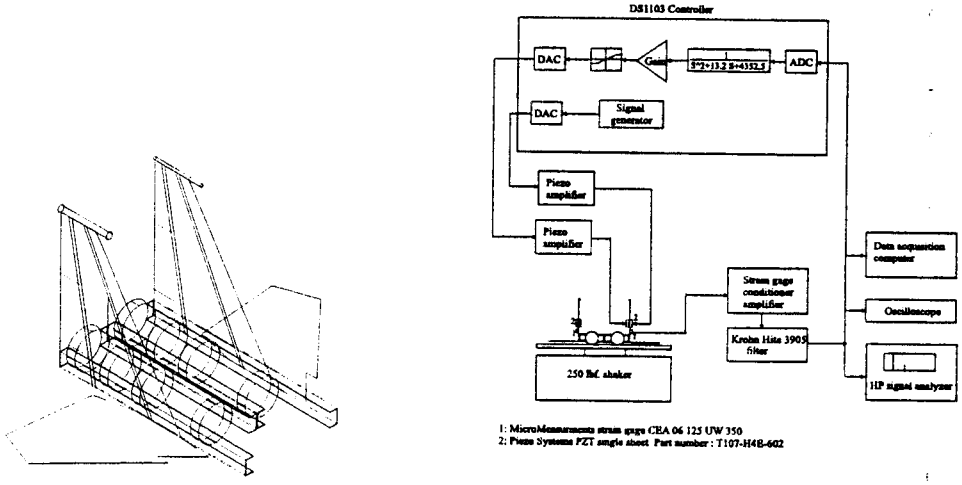

(i) (ii)

Figure 8: (i) Three-dimensional view of the twin-tail assembly, and (ii) experimental setup.

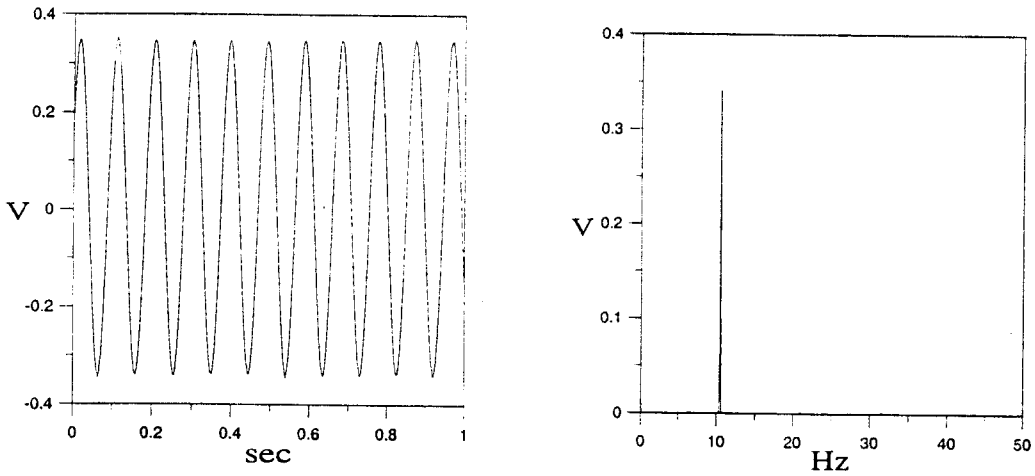

(i) time domain (ii) frequency domain

Figure 9: Response of the open-loop system of the right tail.

response of the tails. To verify the theoretical analysis, we carried out experiments on the structural model of the twin-tail assembly fitted with piezoceramic actuators. We implemented the absorber using a digital signal processing (DSP) device. Good agreement between theory and experiments is found.

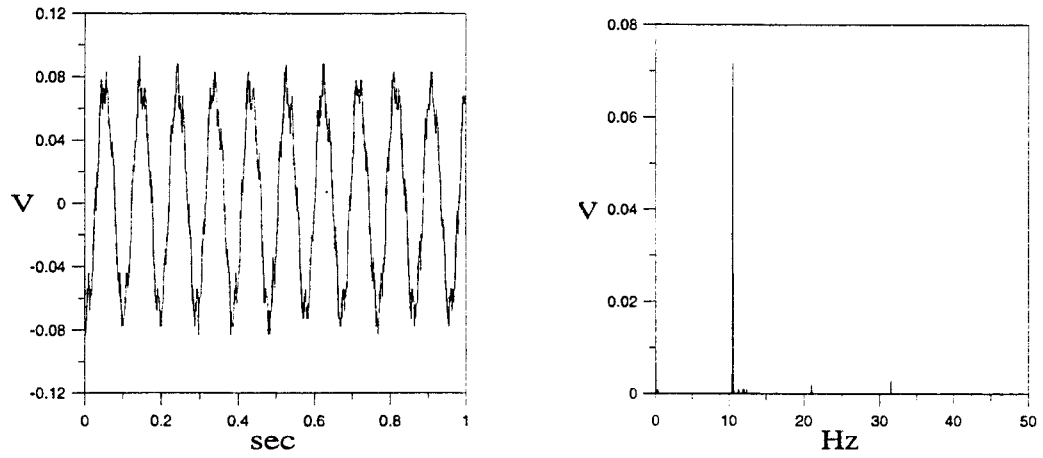

(i) time domain (ii) frequency domain

Figure 10: Response of the closed-loop system of the right tail with quadratic absorber ($\zeta_{3,4} = 0.1$)

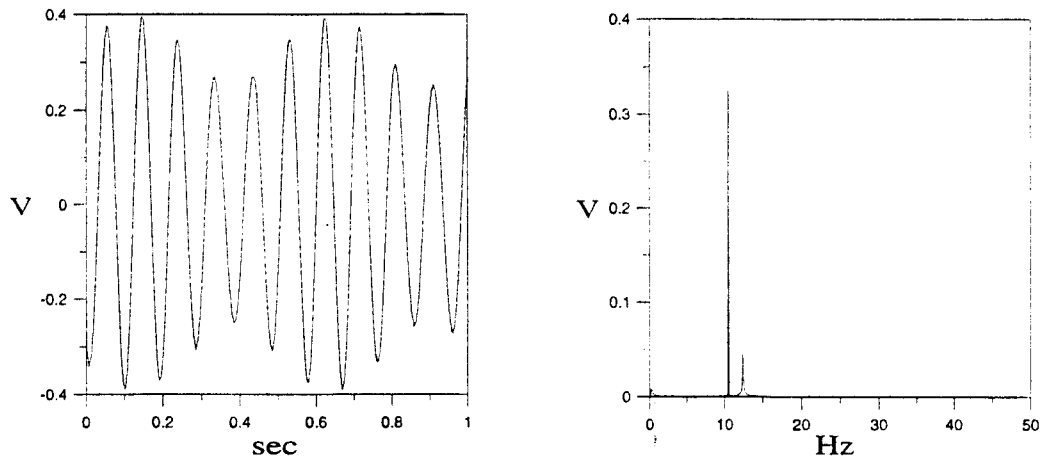

(i) time domain (ii) frequency domain

Figure 11: Control signal.

Appendix I

We estimated the parameters of the model from regressive fits of the experimentally and theoretically determined steady-state response amplitudes. The identified parameters for the right tail are $\omega_1 = 9.135Hz$, $\zeta_1 = 0.01357$, $\mu_3 = 3.157 \times 10^{-4}\mu\epsilon^{-1}$, $\alpha_1 = -3.675 \times 10^{-2}\frac{1}{s^2\mu\epsilon^2}$, and $\eta_1 = 161.54\frac{1}{gs^2}$. The identified parameters

for the left tail are $\omega_2 = 9.05Hz$, $\zeta_2 = 0.01856$, $\mu_4 = 1.958864 \times 10^{-4}\mu\epsilon^{-1}$, $\alpha_2 = -2.977 \times 10^{-3}\frac{1}{s^2\mu\epsilon^2}$, and $\eta_2 = 275.12\frac{1}{gs^2}$. The estimated value for $k = 87(1/sec^2)$.

ACKNOWLEDGEMENTS

This work was supported by the Air Force Office of Scientific Research under Grant No. F496020-98-1-0393.

REFERENCES

1. D. G. Mabey, "Some Aspects of Aircraft Dynamic Loads Due To Flow Separation", *Progress in Aerospace Science*, **26**, pp. 115-151, 1989.
2. C.J. Goh and T.K.Caughey,"On the stability problem caused by finite actuator dynamcis in the collocated control of large space structures," *International Journal of Control*, **41**, pp. 787-802, 1985.
3. J.N.Juang, and M. Phan,"Robust controller designs for second-order dynamic systems: A virtual passive approach," *Journal of Guidance, Control and Dynamics*, **15**, pp. 1192-1198, 1992.
4. M.A. Ferman, S.L. Liguore, C.M. Smith, and B.J. Colvin, "Composite "Exoskin" Doubler Extends F-15 Vertical Tail Fatigue Life", AIAA paper No. 93-1341.
5. A.A. El-Badawy and A.H. Nayfeh, Nonlinear Identification of a Scaled Structural Dynamic Model of the F-15 Tail Section, in: *Proceedings of the 17th International Modal Analysis Conference*, Kissimmee, Fl, pp. 1175-1181, 1999.
6. A.H. Nayfeh, *Introduction to Perturbation Techniques*, Wiley, New York, 1981.
7. A.H. Nayfeh, and B. Balachandran, *Applied Nonlinear Dynamics*, Wiley, New York, 1995.
8. F. Nitzsche, D.G. Zimcik, T.G. Ryall, R.W. Moses and D.A. Henderson, "Control Law Synthesis for Vertical fin Buffet Alleviation Using Strain Actuation," AIAA Paper No. 99-1317.
9. J.J. Hollkamp and T.F. Starchville, Jr., "A self-tuning piezoelectric vibration absorber," *Journal of Intelligent Material Systems and Structures*, **5**, pp. 559-566, 1994.
10. S.S. Oueini, A.H. Nayfeh, "Analysis and Application of a Nonlinear Vibration Absorber", *Journal of Vibration and Control*, accepted for publication, 2000.
11. *SIMULINK: Dynamic System Simulation Software.* Natick, MA: The MathWorks.
12. dSPACE digital signal processing and control engineering GmbH, Paderborn, Germany.